Mechanical efficiency and fatigue of fast and slow muscles of the mouse

C. J. Barclay

Department of Physiology, Monash University, Clayton, Victoria 3168, Australia

1. In this study, the efficiency of energy conversion in skeletal muscles from the mouse was determined before and after a series of contractions that produced a moderate level of fatigue.

2. Initial mechanical efficiency was defined as the ratio of mechanical power output to the rate of initial enthalpy output. The rate of initial enthalpy output was the sum of the power output and rate of initial heat output. Heat output was measured using a thermopile with high temporal resolution.

3. Experiments were performed *in vitro* (25 °C) using bundles of fibres from fast-twitch extensor digitorum longus (EDL) and slow-twitch soleus muscles from mice. Muscles were fatigued using a series of thirty isometric tetani. Initial mechanical efficiency was determined before and again immediately after the fatigue protocol using a series of isovelocity contractions at shortening velocities between 0 and the maximum shortening velocity (V_{max}). Efficiency was determined over the second half of the shortening at each velocity.

4. The fatigue protocol significantly reduced maximum isometric force, V_{max}, maximum power output and flattened the force–velocity curve. The magnitude of these effects was greater in EDL muscle than soleus muscle. In unfatigued muscle, the maximum mechanical efficiency was 0·333 for EDL muscles and 0·425 for soleus muscles. In both muscle types, the fatiguing contractions caused maximum efficiency to decrease. The magnitude of the decrease was 15% of the pre-fatigue value in EDL and 9% in soleus.

5. In a separate series of experiments, the effect of the fatigue protocol on the partitioning of energy expenditure between crossbridge and non-crossbridge sources was determined. Data from these experiments enabled the efficiency of energy conversion by the crossbridges to be estimated. It was concluded that the decrease in initial mechanical efficiency reflected a decrease in the efficiency of energy conversion by the crossbridges.

The function of most skeletal muscles is to convert chemical energy into mechanical energy. This conversion is performed by myosin crossbridges during their cyclic interactions with actin filaments (e.g. Goody & Holmes, 1983). Many activities require skeletal muscles to contract repeatedly for sustained periods of time. The effects of such activity on the mechanical performance of skeletal muscle has been the focus of much research (for recent reviews, see Fitts, 1994; Allen, Lännergren & Westerblad, 1995) but, despite its central role in muscle function, the effect of activity on energy conversion has received little attention. The aim of this study was to determine whether moderate fatigue affects the efficiency of energy conversion in skeletal muscle.

Efficiency can be defined, in general terms, as the ratio of mechanical power output to metabolic power input. The precise definition depends on the metabolic processes encompassed by the term 'metabolic power input'. The ultimate metabolic power source for contraction is ATP hydrolysis but this reaction is rapidly reversed at the expense of phosphocreatine (PCr). Hence, under most conditions, there is no net ATP breakdown and the net biochemical reaction is PCr hydrolysis (for a review, see Woledge, 1971). The time course and extent of PCr hydrolysis can be monitored by measuring the energy (or enthalpy) liberated by the reaction. Energy is liberated from a contracting muscle both as mechanical work and as heat and the rate of energy output is proportional to the rate of PCr hydrolysis. This energy is called 'initial' energy. Energy (as heat) is also produced by the oxidative processes that resynthesize PCr (called 'recovery' heat). In this study, the rate of initial enthalpy output (i.e. energy in addition to any resting and recovery heat production) was calculated and used as an index of metabolic power input.

Some caution is required in equating initial energy, or enthalpy, output to the extent of PCr hydrolysis. Energy balance experiments using frog skeletal muscle, in which the

magnitude of enthalpy output was compared with that expected on the basis of the extent of PCr breakdown, have shown that enthalpy output is greater than can be explained by concomitant PCr hydrolysis both in the early stages of a contraction and also during rapid shortening (for reviews, see Curtin & Woledge, 1978; Woledge, Curtin & Homsher, 1985, pp. 242–268; Homsher, 1987). However, if measurements of enthalpy output are made only after the early 'unexplained' energy has been produced and high shortening velocities are avoided, then enthalpy output is an accurate index of the extent of PCr hydrolysis in frog muscle (Homsher, Yamada, Wallner & Tsai, 1984).

The current study involved determining the efficiency of mouse muscle. The only mammalian muscle which has been used in an energy balance experiment is the slow-twitch soleus muscle from the rat. As in frog muscle, the total enthalpy output from this muscle during a short tetanus exceeded that expected on the basis of concomitant PCr hydrolysis (Gower & Kretzschmar, 1976; Phillips, Takei & Yamada, 1993). However, neither the time course of unexplained energy output nor the effects of shortening velocity on energy balance have been determined for rat soleus. In the absence of such information, in the current investigation it was assumed that the characteristics of energy balance for mouse muscle are the same as those for frog muscle and efficiency was calculated using measurements of enthalpy output that would be expected to reliably reflect the underlying PCr hydrolysis. This was achieved using a contraction protocol in which enthalpy output was measured during shortening that commenced only after a period of isometric contraction during which it would be expected that most of the unexplained enthalpy would have been produced (Homsher *et al.* 1984). In addition, maximum efficiency, the focus of the current study, is typically achieved at velocities between 20 and 30% of maximum shortening velocity (V_{max}) and at these relatively low shortening velocities the entire enthalpy output can be explained by concomitant PCr breakdown (Homsher *et al.* 1984).

Measurement of the rate of enthalpy output has several features that make it an ideal method for an investigation of efficiency and fatigue. First, muscle energetics can be monitored non-destructively, allowing the full relationship between efficiency and shortening velocity to be determined in each muscle in both the non-fatigued and fatigued states. Second, heat production and power output can be measured with sufficiently high temporal resolution that they can both be measured within the time course of shortening. Finally, it is possible to determine the contribution made by crossbridge processes to energy output (Homsher, Mommaerts, Ricchiuti & Wallner, 1972; Smith, 1972) and also to monitor how this contribution varies as fatigue develops (Barclay, Curtin & Woledge, 1993*b*). About one-third of the energy produced during contraction arises from non-crossbridge processes (Homsher *et al.* 1972; Smith, 1972; Barclay *et al.* 1993*b*) and any changes in efficiency that may occur with fatigue could be due to either an alteration in the fraction of enthalpy arising from non-crossbridge sources or to an alteration in the efficiency of energy conversion by the crossbridges. The ability to monitor energy partitioning between crossbridge and non-crossbridge processes as a muscle fatigues allowed these two possible mechanisms to be clearly distinguished.

METHODS

Preparations and solutions

Adult female mice (Swiss strain) were anaesthetized using chloroform and then killed by cervical dislocation. Small bundles of muscle fibres were isolated from the extensor digitorum longus (EDL) and soleus muscles. All animal handling procedures met local ethical requirements. EDL preparations used in the efficiency experiments had a mean (± S.E.M.) dry mass of 1·04 ± 0·05 mg and length of 9·75 ± 0·43 mm ($n = 6$). For soleus preparations ($n = 6$), the corresponding values were 0·87 ± 0·11 mg and 9·87 ± 0·18 mm. During dissection and experiments, muscles were bathed in oxygenated (95% O_2, 5% CO_2) Krebs–Henseleit solution containing (mM): NaCl, 118; KCl, 4·75; $MgSO_4$, 1·18; $NaHCO_3$, 24·8; KH_2PO_4, 1·18; $CaCl_2$, 2·54; glucose, 10. During experiments the temperature of the solution was maintained at 25 °C.

Fibre bundles were attached to the experimental apparatus by T-shaped aluminium clips folded onto each tendon. One clip was glued, using cyanoacrylate adhesive, to a fixed-position mount and the other was attached to a tungsten wire rod that was connected to the arm of a servo-controlled ergometer (Cambridge 300H, Cambridge Technologies, Watertown, MA, USA). Muscles were stimulated via platinum wire electrodes that lightly touched either side of the preparation midway between the ends. Stimulus pulses were of 1 ms duration and ~5 V in amplitude.

Mechanical and thermal recordings

Changes in muscle length and all data recording were controlled using software and a multi-function laboratory interface (Labmaster, Scientific Solutions, Solon, OH, USA.). Muscle length was controlled by software-generated signals sent to the ergometer via a D/A converter at a rate of 1000 Hz. The ergometer was also used to record the time courses of changes in muscle length and force production. All signals were sampled at 500 Hz, digitized, displayed and stored on disk.

The heat measurement technique used has been described in detail previously (Barclay, Arnold & Gibbs, 1995). Briefly, the heat produced by contracting muscles was determined from the rise in muscle temperature. Temperature changes were measured using a thermopile consisting of twenty antimony–bismuth thermocouples spanning 5 mm (Mulieri, Luhr, Trefry & Alpert, 1977; Barclay *et al.* 1995). There were an additional twelve thermocouples, not electrically connected to the recording section, at the end of the thermopile closest to the ergometer. This 'protecting region' ensured that heat loss was uniform along the length of the muscle thus preventing relatively warm regions of muscle moving on to the recording region during shortening (Hill, 1937). The thermopile produced 1·45 mV $°C^{-1}$. Thermopile output was filtered (low-pass filter, cut-off frequency 50 Hz), amplified using a low-noise amplifier (15c-3a, Ancom, Cheltenham, UK), sampled and digitized using a 12-bit A/D converter.

During recording, heat is continually lost from the preparation along the thermocouple wires and into the frame holding the thermopile. The time course of heat loss was exponential and the rate of heat loss was determined by fitting an exponential curve to the signal recorded as a preparation cooled after having been heated using the Peltier effect (Kretzschmar & Wilkie, 1972). Temperature signals were then corrected for heat lost, giving the temperature that would have been reached in the absence of heat losses. Corrected temperature signals were converted to heat by multiplying temperature by the heat capacity of the preparation. The magnitude of this correction was typically between 10 and 15% of the recorded temperature signal after 1 s of contraction. The heat capacity of the part of the preparation over the recording region was determined from the initial rate of cooling after heating the preparation using the Peltier effect (Kretzschmar & Wilkie, 1972). Both heat capacity and changes in muscle temperature were assumed to be uniformly distributed along the preparation (Barclay, Constable & Gibbs, 1993*a*). Some of the increase in muscle temperature during stimulation was due to the stimulus current passing through the muscle. The rate of stimulus heat production was determined by rendering each fibre bundle inexcitable by prolonged depolarization and then measuring the heat produced when the muscle was stimulated using the same stimulus parameters as in the experiment.

Experimental protocols

At the start of each experiment, stimulus voltage was adjusted to ~20% above that required to elicit maximum twitch force. A series of brief tetani were then used to set muscle length. For experiments in which energy partitioning was assessed, only isometric contractions were used and muscle length was set to that at which tetanic force was maximal (L_0). For experiments in which efficiency was determined, isovelocity contractions, in which muscles shortened by ~10% of L_0, were used. In these experiments, muscle length was set ~5% above L_0 so that when muscles shortened, the shortening took place across the plateau region of the force–length relationship.

Fatigue protocol. Muscles were fatigued using a series of thirty isometric tetani, with successive tetani starting at 5 s intervals (Barclay *et al.* 1995). Tetanus duration was chosen (1) to produce a moderate amount of fatigue (i.e. less than 50% decline in isometric force) and (2) to have a similar amount of energy produced in each contraction for both the fast- and slow-twitch muscle types. Durations that met these criteria were 1 s for soleus and 0·2 s for EDL (Barclay *et al.* 1995). Stimulus pulse frequencies were 75 and 125 Hz for soleus and EDL preparations, respectively.

Mechanical efficiency protocol. The relationship between mechanical efficiency and shortening velocity was determined before and after the fatigue protocol using a series of ten isovelocity contractions. In each isovelocity contraction (Fig. 1*A*), muscles initially contracted isometrically. Once isometric force was fully developed, muscle length was decreased at a constant velocity through an amplitude of ~10% L_0. The total contraction duration was 2 s for soleus and 1 s for EDL muscle and shortening commenced after 1 and 0·4 s, respectively. A range of velocities between 0 and V_{max} was used. When determining efficiency prior to the fatiguing contractions, contractions were performed at 1·5 min intervals. The contractions performed after the fatigue protocol were spaced so as to keep the duty cycle (tetanus duration divided by the time between the start of successive tetani) the same as in the preceding, fatigue-producing contractions. Thus isovelocity tetani were performed at 10 s intervals for soleus and

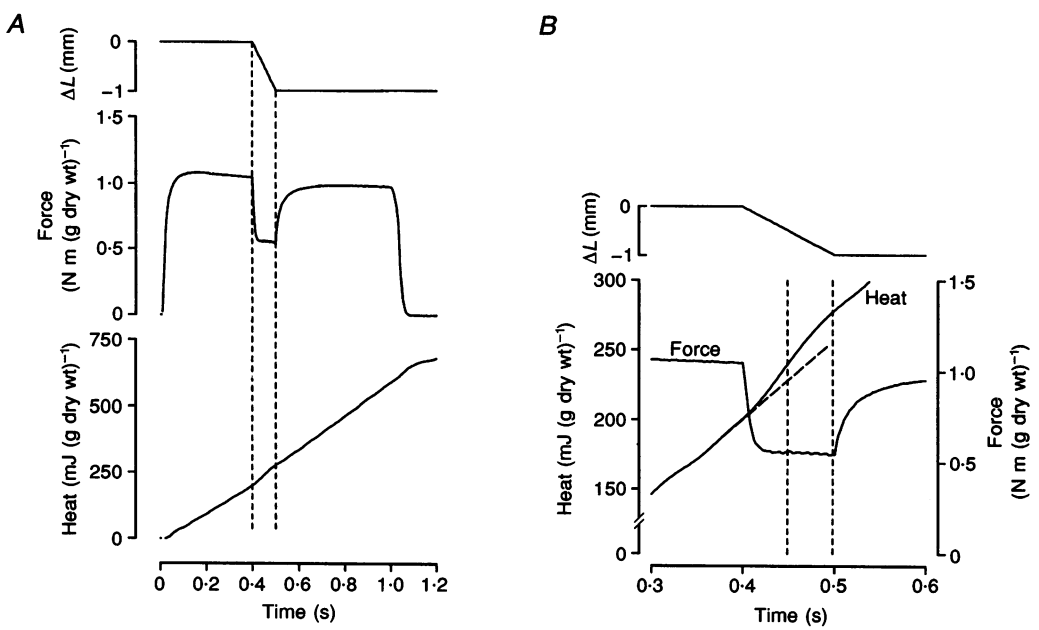

Figure 1. Records illustrating isovelocity contraction protocol and analysis

A, the time course of heat (bottom) and force (middle) output from an EDL fibre bundle during a contraction containing a period of isovelocity shortening. The change in muscle length is shown in the top panel. The duration of shortening is marked by vertical dashed lines. *B*, detailed illustration of the heat and force output during shortening. The vertical dashed lines show the section of the records from which the average power output and rate of heat output were calculated. The angled dashed line is an extrapolation of the isometric heat output prior to shortening.

25 s intervals for EDL. To avoid any consistent effect of order of velocities on the efficiency–velocity relationship, the order of presentation of velocities (either ascending or descending) was varied among preparations. Changes in passive force during each isovelocity contraction were measured by repeating the same pattern of length changes without stimulating the muscles. The force recorded during these events was subtracted from the total force recorded when the muscle was both shortened and stimulated.

Energy partitioning protocol. The energy output from a contracting muscle can be separated into a component that depends on filament overlap, and can thus be attributed to crossbridge interaction with the thin filament, and a component that is largely independent of filament overlap (Homsher *et al.* 1972; Smith, 1972). The latter, called non-crossbridge heat, is thought to be quantitatively dominated by energy used to pump Ca^{2+} into the sarcoplasmic reticulum. Changes in the partitioning of energy use between crossbridge and non-crossbridge sources during the fatigue protocols were studied using a protocol described previously (Barclay *et al.* 1993*b*). Most tetani in the series were performed with muscle length at L_0. It was assumed that at this length overlap between the thick and thin filaments was maximal. At intervals during the series, contractions were performed at a longer muscle length, hence at reduced filament overlap. Filament overlap was reduced in the 2nd, 5th, 10th, 15th, 20th, 25th and 30th tetani. Comparison of the heat produced in pairs of successive tetani, one at full overlap and one at reduced overlap, allowed the division of heat between crossbridge and non-crossbridge sources to be estimated.

To determine the degree of filament overlap, sarcomere length at L_0 was measured in each preparation used for this experiment. At the conclusion of the experiment fibres were fixed, while still on the thermopile, at L_0 using 70% ethanol (Josephson, 1985). The preparations were then removed from the thermopile and kept in ethanol for ~12 h. A few fibres from the region where the heat production had been measured were dissected from the fixed preparation and their sarcomere length was determined from the diffraction pattern formed when light from a laser was shone through the fibres. The mean (± S.E.M.) sarcomere lengths at L_0 were 2·77 ± 0·06 μm for soleus ($n = 6$) and 2·68 ± 0·08 μm for EDL muscle ($n = 6$). Sarcomere length at the long length used in the experiment was determined from the relative increase in total muscle length. The degree of filament overlap was calculated assuming overlap was 100% at L_0 and would be reduced to 0 at a sarcomere length of 3·95 μm (Woledge *et al.* 1985, p. 44). The mean filament overlaps when stretched were 40·3 ± 0·1% for soleus and 31·7 ± 2·3% for EDL ($n = 6$ for both muscle types).

Data analysis

Mechanical efficiency. Mechanical efficiency was defined as the ratio of mechanical power output (i.e. the rate of doing work, $\dot{W}$) to the rate of enthalpy output ($\Delta\dot{H}_i$). The latter is the sum of the rates of heat ($\dot{Q}$) and work output during shortening, $\dot{W} + \dot{Q}$. With regard to the symbols used in this paper, the thermodynamic conventions of symbolizing heat by Q and enthalpy by H have been followed. The average values of $\dot{W}$ and $\dot{Q}$ during the second half of the shortening were calculated (Curtin & Woledge, 1991). Measurements were made over this period to minimize the influence of transient changes in rate of heat production associated with force changes either during the transition from isometric to isovelocity contraction at the start of shortening (Woledge *et al.* 1985, p. 204) or during the redevelopment of isometric force at the end of the shortening (Woledge, Wilson, Howarth, Elzinga & Kometani, 1988). $\dot{W}$ was determined by multiplying the average force produced during the second half of shortening by the velocity of shortening and $\dot{Q}$ was determined from the slope of a straight line fitted through the heat signal recorded during the same period (Fig. 1*B*). Prior to calculating $\dot{Q}$ the heat signal was filtered further using a digital filter implemented in the frequency domain (Press, Flannery, Teukolsky & Vetterling, 1988, pp. 452–454) with a cut-off frequency (−3 dB) of 20 Hz. This removed residual 50 Hz noise from the signal without affecting frequency components of the heat signal which, inspection of the signal power spectrum revealed, were predominantly less than 10 Hz.

The heat measured was that arising from 'initial' chemical reactions with little contribution from oxidative 'recovery' processes. The predominant initial reaction is PCr hydrolysis which occurs while a muscle is contracting. Recovery processes, which regenerate PCr, are relatively slow to commence (Barclay *et al.* 1995) and would have contributed little heat in the pre-fatigue efficiency determinations when the brief contractions were performed at intervals sufficiently long that recovery heat production from one contraction would have been complete before the next began. However, when efficiency was determined immediately after the fatiguing contractions, there was significant recovery heat production occurring during the isovelocity contractions as a result of the preceding series of contractions. The amount of recovery heat produced during each contraction was estimated as described previously (Barclay *et al.* 1995). Recovery heat accounted for < 25% of the total heat output during a contraction. The initial heat was calculated by subtracting the estimated rate of recovery heat from the total rate of heat production during shortening. Thus in both pre- and post-fatigue efficiency determinations, $\dot{Q}$ used to determine mechanical efficiency corresponded to the rate of initial heat output ($\dot{Q}_i$) and thus:

$$\text{Initial mechanical efficiency} = \dot{W}/\Delta\dot{H}_i = \dot{W}/(\dot{W} + \dot{Q}_i).$$

Curve fitting. To accurately describe the relationship between efficiency and shortening velocity, a curve was fitted to the data by combining the mathematical functions used to describe the relationships between both $\dot{W}$ and $\dot{Q}_i$ and shortening velocity. The relationship between $\dot{W}$ and velocity was determined from Hill's (1938) force–velocity curve, fitted using a three-dimensional regression method (Wohlfart & Edman, 1994). The curvature of the force–velocity relationship is described by the parameter a/P_0, where a is the force asymptote of the fitted force–velocity hyperbola and P_0 is the extrapolated maximum isometric force determined from the fitted force–velocity curve. The relationship between $\dot{Q}_i$ and velocity was well described by a straight line (e.g. Fig. 4), which was fitted using a robust linear regression method (Press *et al.* 1988, pp. 562–564).

Data normalization and statistical analysis

At the conclusion of each experiment, muscle length was measured. In experiments in which sarcomere length was not measured, the tendons were then removed from each fibre bundle and the fibres were dried for 24 h. Dry mass was measured using an electronic balance. Rates of energy output were normalized by muscle dry mass and force was normalized by muscle length and dry mass.

The aim of the experiments was to compare, in each muscle type, the maximum mechanical efficiency before and after a series of fatiguing contractions. Student's paired t tests were used to compare maximum isometric force, maximum power, curvature of the force–velocity relationship and maximum mechanical efficiency before and after the fatiguing contractions. Statistical significance was determined with respect to the 95% level of confidence. All data are presented as means ± S.E.M. For paired comparisons, the

mean values of variables before and after the fatigue protocol are shown as well as the mean difference between pre- and post-fatigue values of each variable. Mean differences are expressed as a percentage of the pre-fatigue value.

RESULTS

Effects of fatigue on the force–velocity relationship

The protocol used in this study to determine mechanical efficiency involved measuring both mechanical power output and rate of heat production at a range of shortening velocities. Muscle fatigue is generally defined in terms of the mechanical performance of the muscle, either as a decline in ability to generate isometric force or decreased power output (Allen *et al.* 1995). The force–velocity relationship summarizes mechanical performance so changes in this relationship summarize the effects of the fatigue protocol on the mechanical performance of the muscle. Representative force–velocity curves, determined before and after the fatigue protocol, from an EDL and a soleus preparation are shown in Fig. 2.

The general effects of fatigue on the two muscle types were similar but the magnitude of the effects differed between the two muscle types. In both muscles, P_0 (either measured directly or determined by extrapolation of the force–velocity relationship) was reduced and the magnitude of the reduction was greater for the EDL fibres than for the soleus fibres. Fatigue also lowered V_{max} of the EDL preparation, although the relative decline was less than that in P_0. V_{max} for the soleus preparation decreased by only a small amount. The normalized force–velocity curves (P/P_0 *vs.* V/V_{max}, Fig. 2*B* and *D*) illustrate the change in shape of the curve. The fatigue protocol reduced the curvature of the force–velocity relationship in both muscles but, again, this was more pronounced in the EDL preparation. The curvature of the force–velocity relationship is quantified by the value of a/P_0, which increases in value as the curve flattens. The mean values of P_0, V_{max} and a/P_0 before and after the fatiguing contractions and the relative magnitude of the changes in each variable are given in Table 1. A paired comparison for EDL muscle ($n = 6$) revealed that the thirty 200 ms tetani significantly ($P < 0{\cdot}05$) reduced P_0 and V_{max}

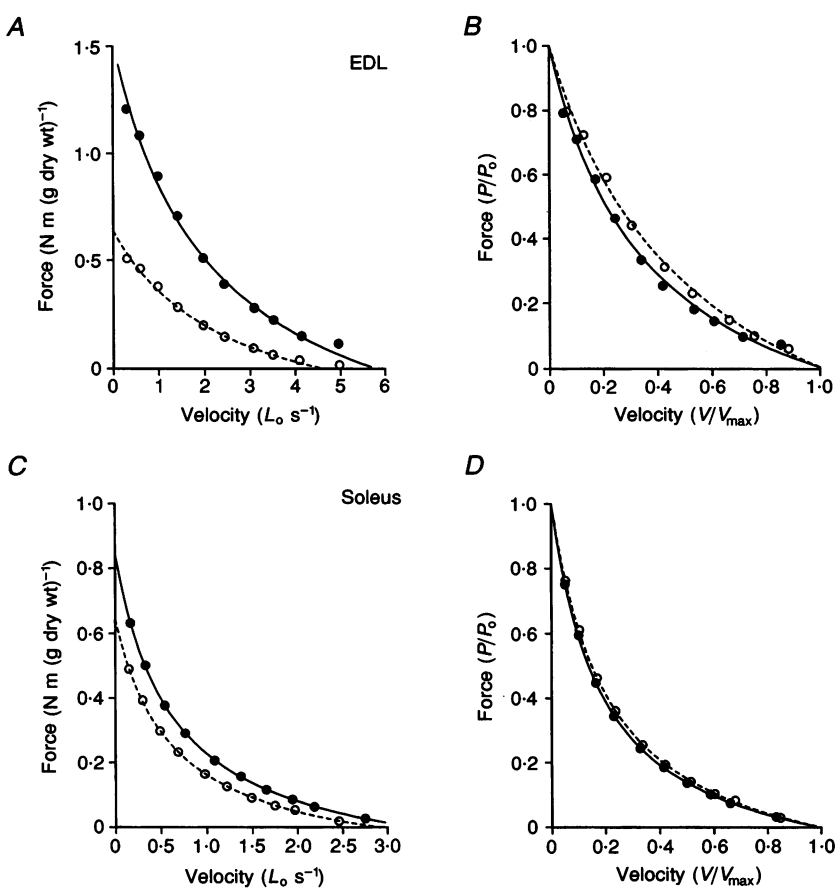

Figure 2. Example of the effects of fatigue on force–velocity properties of EDL and soleus muscles

Force–velocity relationships for fibre bundles from an EDL (*A* and *B*) and a soleus (*C* and *D*) muscle recorded before (●) and after (○) a series of 30 isometric tetani. Data are shown in both absolute units (*A* and *C*) and with force and velocity normalized with respect to P_0 and V_{max} (*B* and *D*), respectively. The data have been fitted with the Hill (1938) force–velocity curve.

Table 1. Effect of fatigue on force–velocity properties of EDL and soleus muscle

	Measured P_0 (N m g^{-1})	Extrapolated P_0 (N m g^{-1})	Extrapolated V_{max} (L_o s^{-1})	a/P_0
	EDL			
Pre-fatigue	1·28 ± 0·15	0·941 ± 0·18	5·61 ± 0·22	0·466 ± 0·057
Post-fatigue	0·72 ± 0·11	0·48 ± 0·08	4·81 ± 0·19	0·648 ± 0·093
Mean difference (% pre-fatigue value)	44·5 ± 3·3*	48·4 ± 2·4*	13·9 ± 1·6*	−41·6 ± 13·9*
	Soleus			
Pre-fatigue	1·01 ± 0·06	0·89 ± 0·17	3·15 ± 0·10	0·163 ± 0·010
Post-fatigue	0·87 ± 0·07	0·69 ± 0·09	2·99 ± 0·16	0·207 ± 0·022
Mean difference (% pre-fatigue value)	13·1 ± 3·2*	19·9 ± 4·8*	5·4 ± 2·5*	−26·8 ± 8·4*

$n = 6$ for each preparation. * Significant difference ($P < 0·05$) for pre-fatigue *vs.* post-fatigue, paired comparison. Dry muscle mass used for normalizing rates of energy output.

and increased a/P_0 (Table 1). For soleus muscle ($n = 6$), thirty 1000 ms tetani also resulted in significant reductions in P_0 and V_{max} and increased a/P_0. The magnitude of each of these changes was smaller in slow-twitch soleus muscle than in fast-twitch EDL muscle.

Effects of fatigue on power output

Power output is the product of force and velocity and thus is zero when velocity is 0 (i.e. isometric contraction) and when force is 0 (i.e. velocity $\geqslant V_{max}$). Maximum power output ($\dot{W}_{max}$) was reduced after the fatiguing contractions, regardless of muscle type (Table 2). $\dot{W}_{max}$ from EDL muscles declined by 55·0 ± 3·9% of its pre-fatigue value and $\dot{W}_{max}$ from soleus muscles declined by 24·3 ± 4·8%. Therefore, as has been observed previously (Curtin & Edman, 1994; Westerblad & Lännergren, 1994), the relative decline in peak power output with fatigue is greater than the decline in either P_0 or V_{max} (Table 1). However, although the absolute power output was reduced, the decreased curvature of the force–velocity relationship means that the normalized maximum power output (i.e. power normalized by the product of P_0 and V_{max}, $\dot{W}_{max}/(P_0 V_{max})$; Woledge *et al.* 1985, p. 49) is increased (Curtin & Edman, 1994). Thus the flattening of the force–velocity curve partially counters the reduction in absolute power output resulting from sustained activity.

In unfatigued EDL muscle, maximum power output was achieved at a shortening velocity of 2·05 ± 0·17 L_o s^{-1} or 36·6 ± 2·8% V_{max}. When fatigued, the absolute velocity at

Table 2. Effect of fatigue on energetics of EDL and soleus muscle

	Interpolated $\dot{W}_{max}$ (mW g^{-1})	Isometric $\dot{Q}_1$ (mW g^{-1})	Max. mechanical efficiency	Max. crossbridge efficiency
	EDL			
Pre-fatigue	671 ± 75	755 ± 100	0·333 ± 0·020	0·384 ± 0·027
Post-fatigue	297 ± 37	400 ± 57	0·282 ± 0·021	0·326 ± 0·024
Mean difference (% pre-fatigue value)	55·0 ± 3·9*	46·8 ± 2·6*	14·9 ± 5·0*	14·4 ± 5·3*
	Soleus			
Pre-fatigue	203·9 ± 8·2	154 ± 13	0·425 ± 0·025	0·482 ± 0·026
Post-fatigue	179·5 ± 10·3	123 ± 11	0·387 ± 0·025	0·441 ± 0·027
Mean difference (% pre-fatigue value)	24·3 ± 4·8*	20·1 ± 3·0*	9·1 ± 1·2*	8·5 ± 1·4*

$n = 6$ for each preparation. * Significant difference ($P < 0·05$) for pre-fatigue *vs.* post-fatigue, paired comparison. Dry muscle mass used for normalizing rates of energy output.

which $\dot{W}$ was maximal was reduced to $1{\cdot}82 \pm 0{\cdot}13$ L_o s^{-1} but the normalized velocity at which $\dot{W}$ was maximal did not differ significantly from that determined in the unfatigued preparations. For soleus preparations, fatigue had no significant effect on either the absolute or normalized velocities at which power output was maximal (pre-fatigue values $0{\cdot}851 \pm 0{\cdot}027$ L_o s^{-1} and $26{\cdot}8 \pm 0{\cdot}4\%$ V_{max}).

The different fatigue protocols for the two muscles were designed so that the amount of initial heat produced in the first tetanus of the protocol was the same in the two muscle types. There was a 5-fold difference between the two muscles in tetanus duration (0·2 *vs.* 1 s) and there was also a 5-fold difference in rate of initial heat output at the start of the series of tetani (Table 2). Thus the 'energy demand' (Barclay *et al.* 1995) was similar in the two muscle types. Despite this energetic matching of the fatigue protocols, the relative changes in P_0, V_{max}, the shape of the force–velocity curve and $\dot{W}_{max}$ were all considerably greater in the fast muscle than in the slow muscle. This is consistent with a previous observation (Barclay *et al.* 1995) that the difference in fatiguability of fast and slow muscles cannot be explained simply on the basis of differences in rate of energy expenditure (or energy demand). Rather, susceptibility to fatigue reflects the ability of a muscle to balance initial energy use with reversal of the initial chemical breakdown by recovery processes.

Effects of fatigue on energetics

Figure 3 shows sections of records of force and heat production that encompass the period during which shortening occurred. These examples show records made using shortening velocities close to that at which initial mechanical efficiency was maximal for each of these preparations. When shortening commenced, force decreased to a new steady level and $\dot{Q}_i$ increased above the steady rate established during the preceding isometric phase of the contraction. Measurements of power output and rate of heat production were made during the second half of shortening. Transient changes in both force and rate of heat production that accompanied the onset of shortening were largely complete within the first half of shortening and when measurements were made both force and the rate of heat production were fairly steady. The effects of fatigue on energetics are summarized in Table 2.

The rate of heat production, given by the slope of the heat records in Fig. 3, during the isometric phase of contraction was reduced by the fatigue protocol. Once again, this effect was greatest in the fast muscle. For EDL preparations ($n = 6$), the magnitude of the reduction in isometric $\dot{Q}_i$ was $46{\cdot}8 \pm 2{\cdot}6\%$ of the rate measured in the unfatigued state. The corresponding value for soleus ($n = 6$) was $20{\cdot}1 \pm 3{\cdot}0\%$. From the records in Fig. 3, $\dot{Q}_i$ from the EDL fibre bundle

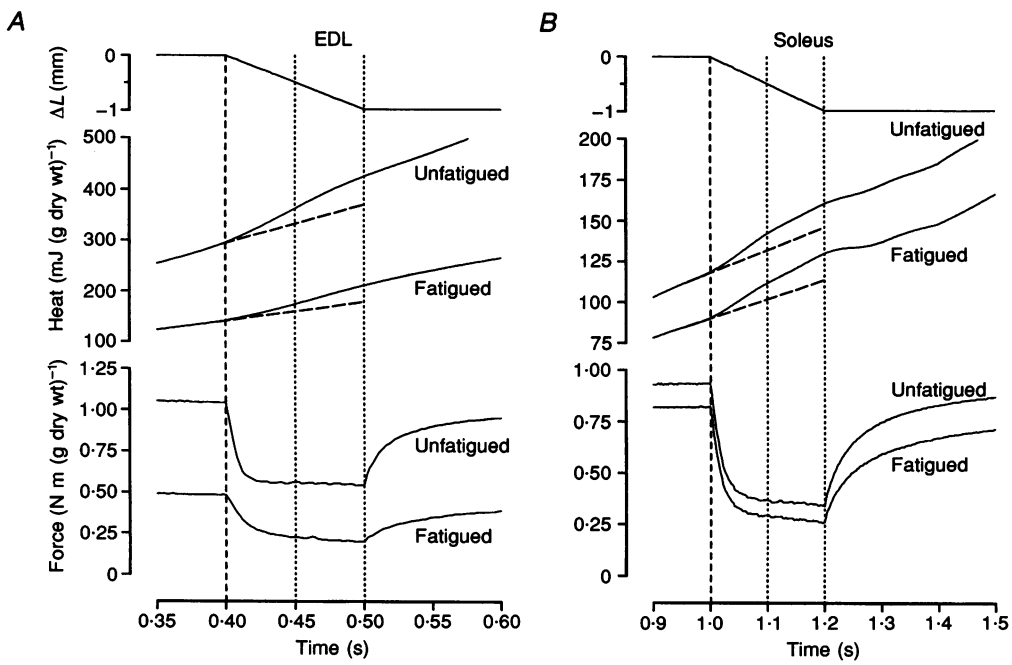

Figure 3. Records of muscle length, force production and heat output in unfatigued and fatigued muscles

Records from isovelocity contractions showing only the section where shortening occurred. For both the EDL (*A*) and soleus (*B*) preparation, shortening velocity was ~20% of unfatigued V_{max}. The vertical dashed lines indicate when shortening started and dotted lines indicate the section of the records from which the average power output and rate of heat output were calculated. The angled dashed lines are an extrapolation of the isometric heat output prior to shortening. Preparation characteristics (total length and dry mass): EDL, 9·5 mm and 1·14 mg; soleus, 9·5 mm and 0·68 mg.

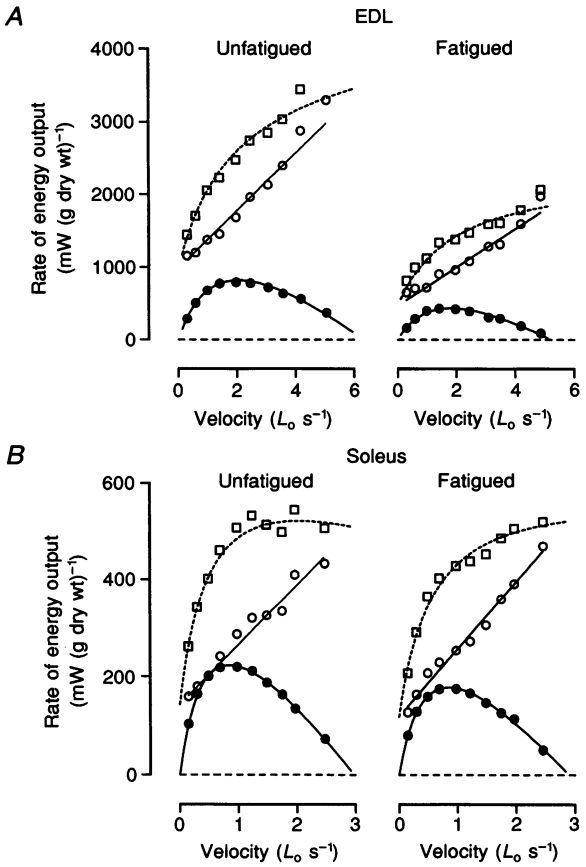

Figure 4. Examples of the effect of fatigue on the relationship between energy output and velocity

Mechanical power output (●) and rates of heat (○) and enthalpy (□) output as a function of velocity of shortening are shown for an EDL (*A*) and soleus preparation (*B*). The data are from the same preparations as in Fig. 2. Data obtained prior to performing 30 tetani are on the left and those obtained immediately after the 30 tetani are on the right. Note the different energy and velocity scales for the two muscle types. Lines are fitted as described in Methods.

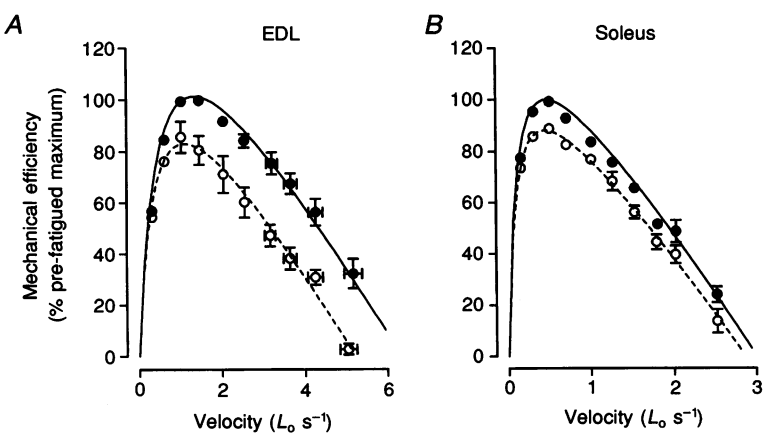

Figure 5. Effect of fatigue on initial mechanical efficiency

Initial mechanical efficiency, expressed relative to the maximum efficiency in the unfatigued state, as a function of shortening velocity before (●) and after (○) a series of 30 isometric tetani. Data are shown for EDL (*A*) and soleus (*B*) muscle. Symbols represent the mean and error bars S.E.M. ($n = 6$ for both EDL and soleus). Shortening velocity is normalized with respect to muscle length (L_o).

during shortening was also reduced in the fatigued state. In contrast, there was little change in $\dot{Q}_i$ from the soleus preparation.

Figure 4 shows an example for each muscle type of the effects of fatigue on the energetic profile of the muscles. During shortening, energy is liberated as mechanical work and as heat, and Fig. 4 shows $\dot{W}$ and $\dot{Q}_i$ as a function of shortening velocity. $\dot{Q}_i$ increased linearly with shortening velocity in both muscle types. Paired comparisons for all the muscles used indicated that in neither muscle type did fatigue significantly affect the slope of the relationship between $\dot{Q}_i$ and shortening velocity although for both muscles the extrapolated isometric $\dot{Q}_i$ (i.e. the y-intercept of the $\dot{Q}_i$ *vs.* V relationship) was significantly lower when the muscles were fatigued.

The rate of enthalpy output ($\Delta\dot{H}_i$; the sum of the power output and rate of heat output) was non-linearly related to shortening velocity with the increment in $\Delta\dot{H}_i$ per unit increase in velocity decreasing as velocity increased. The magnitude of reductions in $\dot{Q}_i$ and $\Delta\dot{H}_i$ with fatigue were markedly greater for EDL preparations than for soleus.

Initial mechanical efficiency and fatigue

Initial mechanical efficiency was calculated by dividing the power output by the rate of initial enthalpy output. Figure 5 illustrates the effect of the fatigue protocol on the relationship between mechanical efficiency and shortening velocity. In the unfatigued state, the maximum efficiency of soleus muscle ($0{\cdot}425 \pm 0{\cdot}025$, $n = 6$) was greater than that of EDL muscle ($0{\cdot}333 \pm 0{\cdot}020$, $n = 6$). After the fatigue protocol, maximum efficiency was significantly reduced in both muscle types. The mean magnitude of the decline in maximum efficiency was $14{\cdot}9 \pm 5{\cdot}0\%$ for EDL preparations and $9{\cdot}1 \pm 1{\cdot}2\%$ for soleus muscles.

Prior to the fatigue protocol, maximum efficiency of EDL muscle was achieved at a mean shortening velocity of $1{\cdot}44 \pm 0{\cdot}03\ L_0\ s^{-1}$ or $25{\cdot}5 \pm 1{\cdot}6\%\ V_{max}$. After the fatigue protocol, the absolute velocity at which efficiency was maximal was significantly reduced (mean value $0{\cdot}99 \pm 0{\cdot}08\ L_0\ s^{-1}$) but there was no significant change in the normalized velocity at which efficiency was maximum ($20{\cdot}7 \pm 2{\cdot}1\%\ V_{max}$ after fatigue). For unfatigued soleus efficiency was maximal at $0{\cdot}475 \pm 0{\cdot}026\ L_0\ s^{-1}$ or $15{\cdot}0 \pm 0{\cdot}1\%\ V_{max}$ and fatigue significantly altered neither the absolute nor normalized velocity of shortening at which efficiency was maximum.

Partitioning of energy expenditure

Muscle power output must arise from the crossbridge processes that generate force and filament sliding. However, $\dot{Q}_i$ includes not only a crossbridge-dependent component but also a component related to non-crossbridge energy consuming processes (Homsher *et al.* 1972; Smith, 1972). The main source of non-crossbridge heat production is ion pumping, in particular the sarcoplasmic reticulum Ca^{2+} pump (reviewed by Homsher & Kean, 1978). As $\dot{Q}_i$ includes a non-crossbridge component, the decrease in initial mechanical efficiency caused by the fatigue protocol does not necessarily reflect changes in the efficiency of crossbridge energy conversion. To estimate the efficiency of crossbridge energy conversion and to determine whether this changed during the fatigue protocol it is necessary to know how

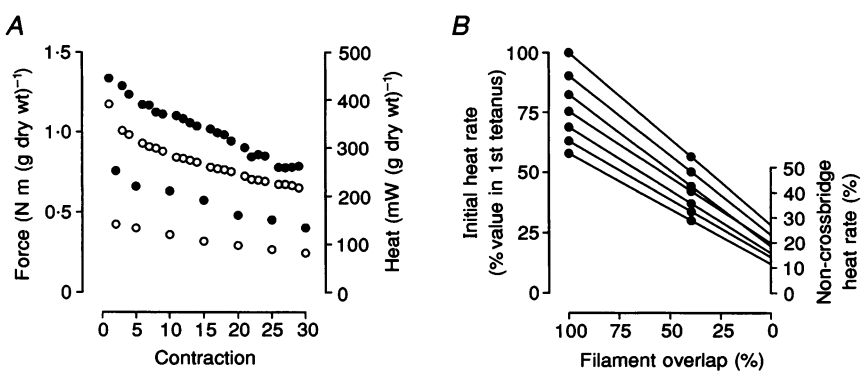

Figure 6. Protocol used to estimate partitioning of energy expenditure between crossbridge and non-crossbridge sources

A, isometric force production (○) and the rate of initial heat output (●) from an EDL preparation for each contraction in a series of thirty 0·2 s tetani. The two lower sets of points are the force and heat rate in contractions performed with filament overlap reduced to 34%. The two upper sets of points were from tetani at full filament overlap. At reduced filament overlap, both isometric force and rate of heat production were reduced. Filament overlap was reduced by increasing muscle length immediately after the preceding contraction performed at full overlap (L_0). Muscle length was returned to L_0 immediately after relaxation was completed. *B*, the contribution to the rate of initial heat output by non-crossbridge processes was estimated from the relationship between initial heat rate and filament overlap. Lines fitted through pairs of data points, recorded from successive tetani, were extrapolated to 0% overlap. The rate of heat output at 0% overlap, expressed as a percentage of the initial heat in the first contraction of the series (performed at L_0), was used as an estimate of non-crossbridge heat rate. The data are from the records shown in *A*.

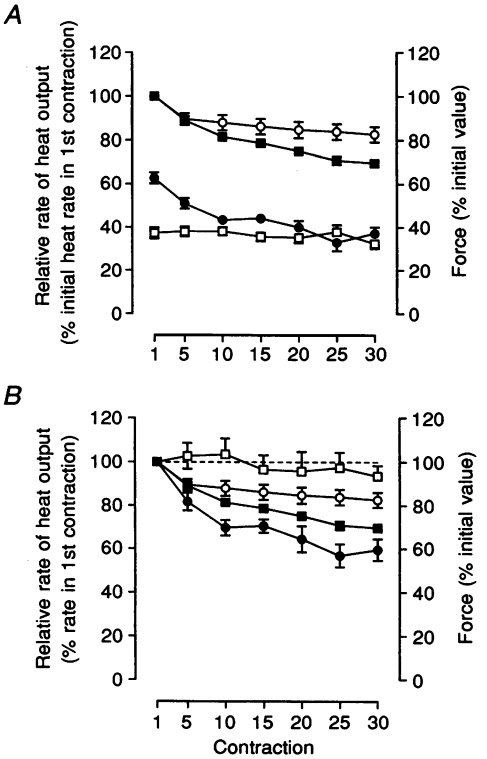

Figure 7. Energy partitioning in soleus muscle during the fatigue protocol

Changes during a series of thirty 1 s isometric tetani in the isometric force recorded at L_o (○), the rate of initial heat output (■) and the estimated rates of heat output from crossbridge (●) and non-crossbridge (□) sources. Symbols represent means ($n = 6$) and error bars S.E.M. Error bars are not shown where they did not exceed the diameter of the symbol. Rates of heat output are shown both relative to the rate of initial heat output in the first contraction of the series (*A*) and also relative to the value of each component in the first contraction (*B*). The horizontal dashed line in *B* marks the 100% (i.e. no change in value) line.

energy expenditure was partitioned between crossbridge and non-crossbridge processes during the fatigue protocol. A series of experiments was performed to determine the energy partitioning. Figure 6 illustrates this protocol and the method of analysis.

Changes in energy partitioning between crossbridge and non-crossbridge processes during the fatigue protocol are shown in Figs 7 (soleus) and 8 (EDL). During the fatigue protocol, the force produced by soleus preparations ($n = 6$) declined to 82·6 ± 3·5% of its initial value and isometric $\dot{Q}_1$

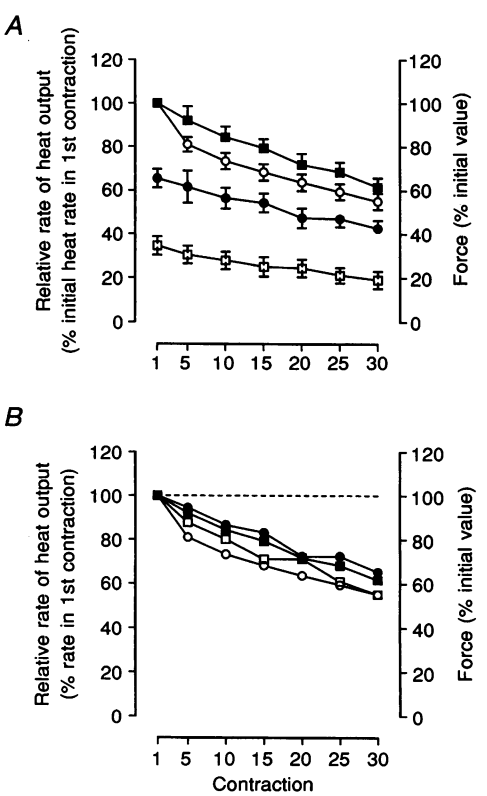

Figure 8. Energy partitioning in EDL muscle during the fatigue protocol

Changes during a series of thirty 0·2 s isometric tetani in the isometric force recorded at L_o (○), the rate of initial heat output (■) and the estimated rates of heat output from crossbridge (●) and non-crossbridge (□) sources. Symbols represent means ($n = 6$) and error bars S.E.M. Rates of heat output are shown both relative to the rate of initial heat output in the first contraction of the series (*A*) and also relative to the value of each component in the first contraction (*B*). The horizontal dashed line in *B* marks the 100% (i.e. no change in value) line.

decreased to 69·6 ± 1·2% of the value in the first contraction ($\dot{Q}_{i(1)}$; Fig. 7*A*). During the fatiguing contractions, there was only a small change in the magnitude of non-crossbridge heat so virtually all the decline in $\dot{Q}_i$ was due to a decline in crossbridge heat (Fig. 7*B*). Crossbridge heat was 62·7 ± 2·6% of $\dot{Q}_{i(1)}$ at the start of the series of contractions and declined to 37·2 ± 2·9% of $\dot{Q}_{i(1)}$ by the end of the fatigue protocol (Fig. 7*A*). Non-crossbridge processes initially accounted for 37·3 ± 2·6% of $\dot{Q}_{i(1)}$ and at the end of the fatiguing tetani was 32·4 ± 2·7% of $\dot{Q}_{i(1)}$ (Fig. 7*A*). Thus by the end of the series of contractions, crossbridge and non-crossbridge processes contributed almost equally to the rate of initial heat output from the soleus preparations during isometric contraction.

For EDL ($n = 6$), during the fatigue protocol isometric force declined to 55·2 ± 3·7% of its initial value and $\dot{Q}_i$ declined to 61·7 ± 4·1% if its initial value (Fig. 8*A*). At the start of the fatigue protocol crossbridge heat corresponded to 65·5 ± 4·2% of $\dot{Q}_{i(1)}$ and non-crossbridge heat 35·4 ± 4·2% of $\dot{Q}_{i(1)}$. During the fatiguing contractions, the magnitudes of both crossbridge and non-crossbridge heat declined significantly to 42·6 ± 3·7% and 19·1 ± 3·9% of $\dot{Q}_{i(1)}$, respectively (Fig. 8*A*). Thus in contrast to the soleus fibre preparations, the relative contributions to $\dot{Q}_i$ of crossbridge and non-crossbridge processes decreased to similar extents (Fig. 8*B*).

The purpose of the energy partitioning experiment was to allow the maximum crossbridge initial efficiency to be estimated. It should also be noted that this 'crossbridge' efficiency is not the thermodynamic efficiency of the crossbridge cycle, power/rate of change in *free energy* (Woledge *et al.* 1985, p. 263) as it was calculated using the initial enthalpy presumed to arise from crossbridge cycling. It should also be noted that the partitioning experiments required the use of isometric contractions whereas the efficiency experiments used isovelocity contractions. Consequently, it is necessary to assume that energy output from non-crossbridge sources is of the same magnitude in both isometric and isovelocity contractions. Making this assumption and using the data obtained from the energy partitioning experiments, the peak initial efficiency of the crossbridges before and after the fatigue protocol was calculated for each fibre preparation used in the efficiency experiments. For both muscles, maximum mechanical efficiency calculated using the rate of enthalpy output presumed to arise just from crossbridge cycling was ~15% higher than that calculated using the measured enthalpy. For example, the estimated maximum crossbridge initial efficiency for unfatigued soleus preparations was 0·482 ± 0·026 compared with a value of 0·425 ± 0·025 calculated using the total initial enthalpy output. However, the magnitude of the decrease in crossbridge mechanical efficiency was the same as the decrease in mechanical efficiency calculated using the rate of total initial enthalpy output (Table 2). Thus combining the results of the efficiency and the energy partitioning experiments indicates that the decrease in initial mechanical efficiency with fatigue reflected decreased efficiency of energy conversion by the crossbridges.

DISCUSSION

These experiments showed that a series of brief tetanic contractions altered not only muscle mechanical performance but also a fundamental aspect of the energetic function of muscle – reducing initial mechanical efficiency. That is, the energy output from fatigued muscle per unit of external work performed was greater than from unfatigued muscle. Furthermore, data obtained from the energy partitioning experiments indicated that the decreased initial mechanical efficiency reflected decreased efficiency of energy conversion by the crossbridges in both fast- and slow-twitch mouse muscle.

In this study, the rate of muscle enthalpy production was used as an index of the rate of the biochemical reactions underlying contraction. Thus an important point to clarify is whether the quantitative relationship between heat output and the extent of PCr hydrolysis remained constant as muscles fatigue.

Effects of fatigue on molar enthalpy of PCr

The molar enthalpy of a reaction can be affected by the chemical environment in which the reaction occurs and this may be of relevance to this study as fatigue is associated with changes in intracellular composition. For example, the products of PCr hydrolysis (Cr and inorganic phosphate, P_i) accumulate and, in some muscles, intracellular pH decreases (reviewed by Fitts, 1994; Allen *et al.* 1995). The enthalpy of PCr hydrolysis (ΔH_{PCr}) is relatively insensitive to accumulation of the products of the reaction but does decrease when pH is lowered (Woledge & Reilly, 1988). Typically, there is little alteration in intracellular pH of slow-twitch muscles during moderately fatiguing contractions (Sahlin, Edström & Sjöholm, 1987). Further support for this idea comes from the small effect of the fatigue protocol used in the current study on V_{max} of soleus muscle (Fig. 2*C*). V_{max} is very sensitive to intracellular pH, with decreases in pH decreasing V_{max} (Curtin & Edman, 1994). However, V_{max} of soleus muscle was only slightly reduced by the fatigue protocol, consistent with the notion that there was probably little change in intracellular pH. In contrast, V_{max} of EDL muscle was markedly reduced by the fatigue protocol and fatigued fast-twitch muscle is characterized by reduced intracellular pH (see review by Fitts, 1994). If pH was reduced in EDL muscles in the current investigation, then ΔH_{PCr} would have also been reduced and efficiency of fatigued EDL muscles would have been overestimated. For example, if intracellular pH decreased by a realistic 0·2 pH units (Sahlin *et al.* 1987), then ΔH_{PCr} would have decreased by 2 kJ mol^{-1} and efficiency would be overestimated by ~5% (i.e. maximum efficiency in fatigued EDL muscle would have been 0·269 rather than 0·282).

Another change in the intracellular environment that both occurs in fatigued muscle and also decreases ΔH_{PCr} is an increase in free Mg^{2+} concentration. However, the concentration of Mg^{2+} has only been observed to increase after prolonged activity and was associated with a large, rapid decline in isometric force (Westerblad & Allen, 1992). The fatigue protocols used in the current study were more moderate than those used by Westerblad & Allen (1992) and no rapid decline in isometric force occurred near the end of the current contraction protocols. Thus it is unlikely that there was any substantial increase in intracellular $[Mg^{2+}]$.

Therefore, the only factor likely to have significantly altered ΔH_{PCr} in fatigued muscles was a decrease in intracellular pH in EDL muscle. This would have caused the magnitude of the decline in efficiency in fast-twitch EDL muscle to be slightly underestimated. This, however, only strengthens the conclusion that initial mechanical efficiency was decreased in moderately fatigued muscle.

Shape of the force–velocity curve and efficiency

An interesting finding was that the fatigue protocols not only decreased the efficiency of energy conversion by the crossbridges but also reduced the curvature of the force–velocity relationship. The possibility that there is a fundamental link between the curvature of the force–velocity relationship and crossbridge efficiency has been proposed on theoretical grounds (Podolsky, 1962; Caplan, 1966) and also on the basis of observations from different types of muscle (Woledge, 1968). The current results are the first demonstration that reducing the curvature of the force–velocity relationship in an individual muscle is associated with a decrease in crossbridge efficiency.

Allen *et al.* (1995) suggested, on the basis of the potential consequences for mechanical performance, that the flattening of the force–velocity curve that occurs with fatigue is of little consequence. However, if the shape of the curve and peak efficiency both reflect the characteristics of a particular step, or steps, in the contraction process, then the change in shape of the curve may reflect changes in muscle function that have considerable energetic consequences.

The basis of a link between the shape of the force–velocity curve and crossbridge efficiency is not known, although Woledge (1968) outlined the probable effects of various alterations in crossbridge function on both efficiency and curvature. To gain some insight into the possible crossbridge basis of the effect of fatigue on the force–velocity properties of muscles in the current study, the data were modelled according to the force–velocity equation of Huxley (1957). This model can be described in terms of three rate constants (Brenner, 1990): f_1, the rate of formation of force-generating crossbridges at positive displacements (i.e. where the relative position of a crossbridge and its binding site on the actin filament are such that crossbridges exert positive force); g_1, the rate constant for transitions into a non-force-generating state in the same region; and g_2, the rate of formation of non-force-generating states in the region where crossbridges produce negative forces and resist filament sliding. The change in shape of the force–velocity relationship for EDL muscle observed in this study was best simulated by assuming that fatigue caused a 6% increase in $f_1 + g_1$ and a 15% decrease in g_2. In these terms, the decreased efficiency would have largely reflected a decrease in net power output due to slower detachment of negatively strained crossbridges. For soleus muscle, the situation was different: the data were best modelled by a 6% decrease in g_2, in accord with the small decrease in V_{max}, and a larger increase (15%) in $(f_1 + g_1)$. For the latter to decrease efficiency would require the predominant change to be an increase in g_1, increasing the probability that a power-producing crossbridge would detach before completing its maximal power-producing cycle. However, such a change would also be expected to increase the ratio of crossbridge heat : isometric force whereas crossbridge heat actually declined considerably more than isometric force in soleus (Fig. 8). So, in terms of this model, it seems likely that the parameter with the most influence on crossbridge efficiency is g_2 and that even small decreases in g_2 have a measurable effect on mechanical efficiency.

Recently, a more complex model of muscle contraction has been formulated (Piazessi & Lombardi, 1995) and this model can predict muscle energetics during shortening more accurately than the original Huxley (1957) model. The newer model incorporates two pathways that crossbridges can follow, each with distinct kinetics and efficiencies. At low shortening velocities, crossbridges predominantly follow a pathway with a short step size, early detachment (i.e. before the amount of filament displacement is sufficient to produce negative strain on the crossbridge) followed by rapid reattachment. This cycle maximizes power output but at the expense of efficiency as free energy is lost in each detachment step. The alternate pathway, which predominates at higher shortening velocities, involves a larger step size, with crossbridges more likely to move into the negative force region, and relatively low rates of reattachment. However, this pathway is also more efficient than the short-step pathway as there are fewer detachments and a smaller free energy drop for each detachment step. In terms of this model, the current finding of decreased efficiency in fatigued muscle and a flatter force–velocity curve (hence increased normalized power output, power/P_0V_0; Curtin & Edman, 1994) could come about if the development of fatigue was accompanied by increased probability of crossbridges progressing through the early detachment, short-step pathway.

Causes of decreased isometric force

This investigation also provides information concerning the basis of the decline in isometric force in the two muscle types. In the soleus muscle, crossbridge-independent heat output did not alter during the contraction protocol (Fig. 7). This has been observed previously in fatigued mouse soleus

(Crow & Kushmerick, 1983) and, if it is assumed that pumping of Ca^{2+} into the sarcoplasmic reticulum dominates crossbridge-independent energy output, then this indicates that a reduction in intracellular Ca^{2+} concentration was unlikely to underlie the decrease in isometric force production in this muscle. This suggests either (or both) the maximum Ca^{2+}-activated force decreased with fatigue or that the relationship between force and Ca^{2+} was shifted to the right by the fatigue protocol. Increased concentrations of H^+ and P_i have these two effects on skinned muscle fibres and probably on intact fibres too (reviewed by Allen *et al.* 1995). As raised intracellular H^+ is not a characteristic of moderately fatigued slow muscle (Sahlin *et al.* 1987), the most likely proposition is that increased P_i accounted for the decrease in force production during the fatigue protocol.

In contrast to soleus muscle, crossbridge-independent heat output from EDL muscle decreased in proportion to the decrease in isometric force (Fig. 8*B*), consistent with the notion that the progressive decline in isometric force production mirrored a decline in intracellular Ca^{2+} concentration as the fatigue protocol progressed (Westerblad & Allen, 1991). It should be noted, however, that a previous study using similar contraction protocols demonstrated that in both muscles the magnitude of force decline was related to the mismatch between energy 'demand' and 'supply' (Barclay *et al.* 1995). So, if the force decline did reflect a reduced influx of Ca^{2+} then the cause of the reduced influx is most probably related to the imbalance between cellular energy use and production. However, although a decrease in Ca^{2+} influx may explain a decrease in force production by EDL muscle, it cannot explain the concomitant decrease in efficiency, so additional factors must have directly affected crossbridge energy conversion.

Conclusion

In conclusion, a series of moderately fatiguing contractions reduced the efficiency of energy conversion by both fast- and slow-twitch skeletal muscle of the mouse. This change was associated with a flattening of the force–velocity relationship, which means an increased normalized power output. The combination of increased normalized power and decreased efficiency suggests that in moderately fatigued muscle power output is optimized at the expense of efficiency.

Allen, D. G., Lännergren, J. & Westerblad, H. (1995). Muscle cell function during prolonged activity: cellular mechanisms of fatigue. *Experimental Physiology* **80**, 497–527.

Barclay, C. J., Arnold, P. D. & Gibbs, C. L. (1995). Fatigue and heat production in repeated contractions of mouse skeletal muscle. *Journal of Physiology* **488**, 741–752.

Barclay, C. J., Constable, J. C. & Gibbs, C. L. (1993*a*). Energetics of fast- and slow-twitch muscles of the mouse. *Journal of Physiology* **472**, 61–80.

Barclay, C. J., Curtin, N. A. & Woledge, R. C. (1993*b*). Changes in crossbridge and non-crossbridge energetics during moderate fatigue of frog muscle fibres. *Journal of Physiology* **468**, 543–555.

Brenner, B. (1990). Muscle mechanics and biochemical kinetics. In *Molecular Mechanisms in Muscular Contraction*, ed. Squire, J. M., pp. 77–149. Macmillan, London.

Caplan, S. R. (1966). A characteristic of self-regulated linear energy converters. The Hill force–velocity relation for muscle. *Journal of Theoretical Biology* **11**, 63–86.

Crow, M. T. & Kushmerick, M. J. (1983). Correlated reduction of velocity of shortening and rate of energy utilization in mouse fast-twitch muscle during continuous tetanus. *Journal of General Physiology* **82**, 703–720.

Curtin, N. A. & Edman, K. A. P. (1994). Force–velocity relation for frog muscle fibres: effects of moderate fatigue and of intracellular acidification. *Journal of Physiology* **475**, 483–494.

Curtin, N. A. & Woledge, R. C. (1978). Energy changes and muscular contraction. *Physiological Reviews* **58**, 690–761.

Curtin, N. A. & Woledge, R. C. (1991). Efficiency of energy conversion during shortening of muscle fibres from the dogfish *Scyliorhinus canicula*. *Journal of Experimental Biology* **158**, 343–353.

Fitts, R. A. (1994). Cellular mechanisms of muscle fatigue. *Physiological Reviews* **74**, 49–94.

Goody, R. S. & Holmes, K. C. (1983). Cross-bridges and the mechanism of muscle contraction. *Biochimica and Biophysica Acta* **726**, 13–39.

Gower, D. & Kretzschmar, K. M. (1976). Heat production and chemical change during isometric contraction of rat soleus muscle. *Journal of Physiology* **258**, 659–671.

Hill, A. V. (1937). Methods of analysing the heat production of muscle. *Proceedings of the Royal Society of London* B **124**, 114–136.

Hill, A. V. (1938). The heat of shortening and the dynamic constants of muscle. *Proceedings of the Royal Society of London* B **126**, 136–195.

Homsher, E. (1987). Muscle enthalpy production and its relationship to actomyosin ATPase. *Annual Review of Physiology* **49**, 673–690.

Homsher, E. & Kean, C. J. (1978). Skeletal muscle energetics and metabolism. *Annual Review of Physiology* **40**, 93–131.

Homsher, E., Mommaerts, W. F. H. M., Ricchiuti, N. V. & Wallner, A. (1972). Activation heat, activation metabolism and tension-related heat in frog semitendinosus muscles. *Journal of Physiology* **220**, 601–625.

Homsher, E., Yamada, T., Wallner, A. & Tsai, J. (1984). Energy balance studies in frog skeletal muscle shortening at one-half maximal shortening velocity. *Journal of General Physiology* **84**, 347–359.

Huxley, A. F. (1957). Muscle structure and theories of contraction. *Progress in Biophysics and Biophysical Chemistry* **7**, 255–318.

Josephson, R. K. (1985). Mechanical power output from striated muscle during cyclic contraction. *Journal of Experimental Biology* **114**, 493–512.

Kretzschmar, K. M. & Wilkie, D. R. (1972). A new method for absolute heat measurements using the Peltier effect. *Journal of Physiology* **224**, 18–21*P*.

Mulieri, L. A., Luhr, G., Trefry, J. & Alpert, N. R. (1977). Metal film thermopiles for use with rabbit right ventricular papillary muscles. *American Journal of Physiology* **233**, C146–156.

Phillips, S. K., Takei, M. & Yamada, K. (1993). The time course of phosphate metabolites and intracellular pH using ^{31}P NMR compared to recovery heat in rat soleus muscle. *Journal of Physiology* **460**, 693–704.

PIAZESSI, G. & LOMBARDI, V. (1995). A cross-bridge model that is able to explain mechanical and energetic properties of shortening muscle. *Biophysical Journal* **68**, 1966–1979.

PODOLSKY, R. J. (1962). Mechanochemical basis of muscular contraction. *Federation Proceedings* **21**, 964–974.

PRESS, W. H., FLANNERY, B. P., TEUKOLSKY, S. A. & VETTERLING, W. T. (1988). *Numerical Recipes in C.* Cambridge University Press, Cambridge, UK.

SAHLIN, K., EDSTRÖM, L. & SJÖHOLM, H. (1987). Force, relaxation and energy metabolism of rat soleus muscle during anaerobic contraction. *Acta Physiologica Scandinavica* **129**, 1–7.

SMITH, I. C. H. (1972). Energetics of activation in frog and toad muscle. *Journal of Physiology* **220**, 583–599.

WESTERBLAD, H. & ALLEN, D. G. (1991). Changes in myoplasmic calcium concentration during fatigue in single mouse muscle fibres. *Journal of General Physiology* **98**, 615–635.

WESTERBLAD, H. & ALLEN, D. G. (1992). Myoplasmic free Mg^{2+} concentration during repetitive stimulation of single fibres from mouse skeletal muscle. *Journal of Physiology* **453**, 413–434.

WESTERBLAD, H. & LÄNNERGREN, J. (1994). Changes of the force–velocity relation, isometric tension and relaxation rate during fatigue in intact single fibres of *Xenopus* skeletal muscle. *Journal of Muscle Research and Cell Motility* **15**, 287–298.

WOHLFART, B. & EDMAN, K. A. P. (1994). Rectangular hyperbola fitted to muscle force–velocity data using three dimensional regression analysis. *Experimental Physiology* **79**, 235–239.

WOLEDGE, R. C. (1968). The energetics of tortoise muscle. *Journal of Physiology* **197**, 685–707.

WOLEDGE, R. C. (1971). Heat production and chemical change in muscle. *Progress in Biophysics & Molecular Biology* **22**, 37–74.

WOLEDGE, R. C., CURTIN, N. A. & HOMSHER, E. (1985). *Energetic Aspects of Muscle Contraction.* Academic Press, London.

WOLEDGE, R. C. & REILLY, P. J. (1988). Molar enthalpy change for hydrolysis of phosphorylcreatine under conditions in muscle cells. *Biophysical Journal* **54**, 97–104.

WOLEDGE, R. C., WILSON, M. G. A., HOWARTH, J. V., ELZINGA, G. & KOMETANI, K. (1988). The energetics of work and heat production by single muscle fibres from the frog. In *Molecular Mechanisms of Muscle Contraction*, ed. SUGI, H. & POLLACK, G., pp. 677–688. Plenum, New York.

Acknowledgements

This work was supported by grants from the National Health and Medical Research Council of Australia and the Australian Research Council. I thank Dr J. West for useful comments on the manuscript.

Author's email address

C. J. Barclay: chris.barclay@med.monash.edu.au

Received 16 April 1996; accepted 11 September 1996.